Int. J. Multiphase Flow Vol. 14, No. 5, pp. 633–643, 1988
Printed in Great Britain.

0301-9322/88 $3.00 + 0.00

PLANE TWO-PHASE STAGNATION-POINT FLOW ABOVE A STRETCHING SHEET

K. NIKAIEN and J. PEDDIESON JR
Tennessee Technological University, Cookeville, TN 38505, U.S.A.

(*Received* 13 *January* 1988; *in revised form* 14 *April* 1988)

Abstract—The steady-state two-dimensional flow which takes place in a half space of two-phase suspension bounded by an infinite stretching sheet is investigated. This problem is used as a vehicle for the study of certain aspects of two-phase stagnation-point flow. Attention is focused on the singularity in the particle-phase density distribution in the vicinity of the stagnation point predicted by certain existing theories. It is found that the inclusion of a particle-phase pressure gradient in the governing equations eliminates singular behavior in the particle-phase density distribution and makes possible the calculation of stagnation-point solutions throughout the entire range of inverse Stokes numbers.

Key Words: solid–liquid flow, two-phase stagnation-point flow, dusty gas, boundary layer

INTRODUCTION

Two-phase particulate–suspension flows containing fluid-phase stagnation points occur whenever a blunt solid body is immersed in a two-phase stream. Flow fields of this kind are of interest in connection with applications involving dust-collection equipment, gas masks, turbine-blade erosion, missile-radome erosion and aircraft icing. In addition, stagnation-point flow is a basic problem in fluid mechanics and, for this reason, is of intrinsic interest.

Many types of flow fields contain stagnation points. This paper is concerned with one of these, namely the two-dimensional flow which takes place in a half space of suspension bounded by an infinite sheet stretching parallel to itself in such a way that the speed of any point is directly proportional to the distance of that point from the one fixed line in the sheet. While this problem has no direct relevance to the applications discussed above, it is felt (for reasons to be explained later) that it is a useful model problem for the investigation of two-phase stagnation-point phenomena. A more detailed discussion of the problem under consideration herein is greatly facilitated by access to the governing equations. For this reason such discussion will be deferred to the next section.

GOVERNING EQUATIONS

Consider the steady flow of a two-phase fluid–particle suspension. The mass-balance equations for the two phases can be written in the forms

$$\nabla\cdot((1-\alpha)\mathbf{v}_c) = 0 \qquad [1a]$$

and

$$\nabla\cdot(\alpha\mathbf{v}_d) = 0, \qquad [1b]$$

where ∇ is gradient operator, $\mathbf{v}_c$ is the fluid-phase (continuous-phase) velocity, $\mathbf{v}_d$ is the particle-phase (dispersed-phase) velocity, and $\alpha = \alpha_d$ is the particle-phase volume fraction (the fluid-phase volume fraction being $\alpha_c = 1-\alpha$). The linear-momentum-balance equations can be written (neglecting gravity) in the forms

$$\rho_c(1-\alpha)\mathbf{v}_c\cdot\nabla\mathbf{v}_c = -\nabla((1-\alpha)p_c) + \nabla\cdot((1-\alpha)\boldsymbol{\sigma}_c) - \mathbf{f} \qquad [2a]$$

and

$$\rho_d\alpha\mathbf{v}_d\cdot\nabla\mathbf{v}_d = -\nabla(\alpha p_d) + \nabla\cdot(\alpha\boldsymbol{\sigma}_d) + \mathbf{f}, \qquad [2b]$$

where ρ_c is the fluid density, ρ_d is the particle density, p_c is the fluid-phase pressure, p_d is the

particle-phase pressure, σ_c is the fluid-phase extra-stress tensor, σ_d is the particle-phase extra-stress tensor and $\mathbf{f}$ is the interphase force per unit volume.

It is desired to concentrate herein on situations involving small volume fractions ($\alpha \ll 1$). The dusty-gas equations [see, for instance, Marble (1970)] are normally used for this purpose. In the present work a slight generalization of the dusty-gas equations will be employed. This generalization is most easily achieved by supplementing the balance laws by the assumption $\alpha \ll 1$ and the constitutive equations

$$p_d = p_c = p, \tag{3a}$$

$$\sigma_c = \mu_c(\nabla \mathbf{v}_c + \nabla \mathbf{v}_c^T), \tag{3b}$$

$$\sigma_d = 0 \tag{3c}$$

and

$$\mathbf{f} = \rho_d N \alpha(\mathbf{v}_c - \mathbf{v}_d) + p\nabla\alpha, \tag{3d}$$

where μ_c is the fluid dynamic viscosity and N is an interphase momentum-transfer coefficient (both assumed constant in the present work). In writing [3a–d] it is assumed that a single-pressure model is adequate, that the fluid-phase extra stress follows Newton's law of viscosity, that the particle-phase extra stress is negligible and that the interphase force can be treated as a superposition of steady-state drag (first term) and buoyancy (second term). Substitution of [3a–d] into [1a, b] and [2a, b] and the use of the assumption $\alpha \ll 1$ results in the following set of equations:

$$\nabla \cdot \mathbf{v}_c = 0, \tag{4a}$$

$$\mathbf{v}_c \cdot \nabla \mathbf{v}_c = \frac{-\nabla p}{\rho_c} + \nu_c \nabla^2 \mathbf{v}_c + N\left(\frac{\rho_d}{\rho_c}\right)\alpha(\mathbf{v}_d - \mathbf{v}_c), \tag{4b}$$

$$\nabla \cdot (\alpha \mathbf{v}_d) = 0 \tag{4c}$$

and

$$\mathbf{v}_d \cdot \nabla \mathbf{v}_d = -\frac{\nabla p}{\rho_d} + N(\mathbf{v}_c - \mathbf{v}_d), \tag{4d}$$

where $\nu_c = \mu_c/\rho_c$ is the fluid kinematic viscosity.

It will be convenient to nondimensionalize [4a–d] using a characteristic length L, a characteristic velocity V and a characteristic volume fraction Λ. Substituting

$$\nabla = \overset{*}{\nabla}/L, \tag{5a}$$

$$\mathbf{v}_c = V\overset{*}{\mathbf{v}}_c, \tag{5b}$$

$$\mathbf{v}_d = V\overset{*}{\mathbf{v}}_d, \tag{5c}$$

$$p = \rho_c V^2 \overset{*}{p} \tag{5c}$$

and

$$\alpha = \Lambda \overset{*}{\alpha} \tag{5d}$$

into [4a–d] (asterisks denoting dimensionless quantities) and dropping the asterisks from the final results for simplicity yields the dimensionless equations

$$\nabla \cdot \mathbf{v}_c = 0, \tag{6a}$$

$$\mathbf{v}_c \cdot \nabla \mathbf{v}_c = -\nabla p + \frac{\nabla^2 \mathbf{v}_c}{R} + \kappa\lambda\alpha(\mathbf{v}_d - \mathbf{v}_c), \tag{6b}$$

$$\nabla \cdot (\alpha \mathbf{v}_d) = 0 \tag{6c}$$

and

$$\mathbf{v}_d \cdot \nabla \mathbf{v}_d = -\epsilon \nabla p + \lambda(\mathbf{v}_c - \mathbf{v}_d), \tag{6d}$$

where

$$R = \frac{VL}{\nu_c}, \tag{7a}$$

$$\epsilon = \frac{\rho_c}{\rho_d}, \tag{7b}$$

$$\kappa = \frac{\Lambda \rho_d}{\rho_c} = \frac{\Lambda}{\epsilon} \tag{7c}$$

and

$$\lambda = \frac{NL}{V} \tag{7d}$$

are the Reynolds number, the density ratio, the particle loading and the inverse Stokes number, respectively. Two special cases of [6a–d] will be of interest in the present work. They will be discussed next. To distinguish the complete equations [6a–d] from the following special cases, [6a–d] will be called the modified dusty-gas equations.

If ϵ is formally equated to zero in [6a–d] one obtains the equation set

$$\nabla \cdot \mathbf{v}_c = 0, \tag{8a}$$

$$\mathbf{v}_c \cdot \nabla \mathbf{v}_c = -\nabla p + \frac{\nabla^2 \mathbf{v}_c}{R} + \kappa\lambda\alpha(\mathbf{v}_d - \mathbf{v}_c), \tag{8b}$$

$$\nabla \cdot (\alpha \mathbf{v}_d) = 0 \tag{8c}$$

and

$$\mathbf{v}_d \cdot \nabla \mathbf{v}_d = \lambda(\mathbf{v}_c - \mathbf{v}_d). \tag{8d}$$

These are the dusty-gas equations discussed by Marble (1970) and employed in a variety of previous investigations. If, in addition, κ is formally equated to zero one has

$$\nabla \cdot \mathbf{v}_c = 0, \tag{9a}$$

$$\mathbf{v}_c \cdot \nabla \mathbf{v}_c = -\nabla p + \frac{\nabla^2 \mathbf{v}_c}{R}, \tag{9b}$$

$$\nabla \cdot (\alpha \mathbf{v}_d) = 0 \tag{9c}$$

and

$$\mathbf{v}_d \cdot \nabla \mathbf{v}_d = \lambda(\mathbf{v}_c - \mathbf{v}_d). \tag{9d}$$

Equations [9a, b] are recognized as the usual Navier–Stokes equations for a Newtonian fluid. Thus, to the order of approximation inherent in [9a–d], the presence of particles does not affect the motion of the fluid. The fluid motion can be found first and then [9c, d] can be solved to find the particle motion and volume-fraction distribution associated with the known fluid flow field. Equation [9d] is solved first to find the particle-phase velocity field and then [9c] is solved to find the particle-phase volume-fraction distribution. In the present paper [9a–d] will be called the dilute dusty-gas equations.

Before continuing, some brief comments on the physical meanings of the limiting cases discussed above are in order. Naturally none of the quantities ϵ, κ and Λ can ever be exactly zero. The dusty-gas equations are meant to describe situations in which ϵ is small, and, in addition, Λ is small but $\kappa = \Lambda/\epsilon$ is finite. Thus the particle-to-fluid density ratio is large but the reference volume fraction is small enough to render the particle loading finite. For a fixed particle-to-fluid density ratio it is obvious that a sufficiently small reference volume fraction will make the particle loading small. This is the situation which the dilute dusty-gas equations are intended to model. One would expect the dusty-gas model to acurately describe suspensions of solid particles or liquid drops in gases as long as the volume fraction is small. The present paper provides an interesting example of a situation in which a small term (the term multiplied by ϵ in [6d]) has an important qualitative effect on predictions.

A variety of investigators have applied equations equivalent to [9a–d] (often with [9d] written in Lagrangian form) to stagnation-point problems. [For an early example see Taylor (1940).] A

general result of these investigations, independent of specific geometry, is that above a certain critical value of λ particles do not strike the body surface in the vicinity of the stagnation point. Most work has concentrated on the solution of [9d]. Recently, solutions of [9c] have been obtained and it has been pointed out by such investigators as Michael (1968), Peddieson (1973, 1976), De la Mora & Rosner (1981) and De la Mora (1982), that as λ approaches the critical value α at the wall becomes increasingly large and, in fact, is predicted to be infinite for λ greater than or equal to the critical value. In fact, of course, α cannot exceed $\alpha_{max} < 1$, the maximum value for which fluid-like behavior would be exhibited. This suggests that it is not possible to employ [9a–d] for the solution of stagnation-point problems. The purpose of the present work is to investigate this matter through the application of [6a–d] and [8a–d] to the geometry described at the beginning of this section.

For this geometry an exact reduction to ordinary differential equations is possible [similar to the reductions employed by Zung (1969) and Ungarish & Greenspan (1983) in their work on two-phase flow near a rotating disk], the boundary conditions far from the sheet can be stated unambiguously, and a closed-form solution for the corresponding single-phase problem has been reported by Crane (1970). All of the above features make this a useful model problem for the investigation of two-phase stagnation-point flow.

The most important practical applications involving stagnation points occur in areas such as dust collection and rain erosion and concern flows past blunt bodies. The application of the dilute dusty-gas equations to these situations is inhibited by the existence of the singularity in the dust-phase volume fraction referred to previously. It is desired herein to investigate whether the use of more sophisticated governing equations can eliminate this singularity. To directly apply [6a–d] to blunt-body problems would require the solution of several coupled partial differential equations and, thus, a large amount of numerical work. A boundary-layer approach (which would allow a boundary-layer stagnation-point problem to be formulated in terms of ordinary differential equations) would not be effective because the determination of the inviscid flow (which is not irrotational) would still require the numerical solution of several coupled partial differential equations. The case of flow against an infinite stationary plane suggests itself as a useful model problem because an exact reduction to ordinary differential equations is possible (De la Mora & Rosner 1981; De la Mora 1982) but the solution thus obtained is a local one and this creates ambiguities when it comes to formulating the boundary conditions far from the plane. (It should be pointed out that some of the difficulties mentioned above do not exist for $\kappa = 0$, but it was specifically desired to investigate the case of $\kappa \neq 0$ in this work.) It is for these reasons that the stretching-sheet geometry was chosen as the most suitable model problem for this investigation of the structure of the governing equations for particulate suspensions exhibiting small volume fractions.

To reduce [6a–d] to ordinary differential equations the following transformations are used (with $\mathbf{e}_x$ and $\mathbf{e}_y$ being unit vectors associated with the x- and y-directions, respectively):

$$L = \left(\frac{\nu_c}{a}\right)^{1/2}, \quad V = (\nu_c a)^{1/2}, \tag{10a, b}$$

$$\Lambda = \alpha_\infty, \quad x = \xi, \quad y = \eta, \tag{10c–e}$$

$$\mathbf{v}_c = \mathbf{e}_x \xi F_c(\eta) + \mathbf{e}_y G_c(\eta), \tag{10f}$$

$$\mathbf{v}_d = \mathbf{e}_x \xi F_d(\eta) + \mathbf{e}_y G_d(\eta), \tag{10g}$$

$$p = H(\eta) \quad \text{and} \quad \alpha = Q_d(\eta), \tag{10h, i}$$

where α_∞ is the volume fraction far from the sheet and a is the ratio of the velocity of a point on the sheet to its distance from the origin. Substituting [10a–i] into [6a–d] results in

$$G_c' + F_c = 0, \tag{11a}$$

$$F_c'' - G_c F_c' - F_c^2 + \kappa\lambda Q_d(F_d - F_c) = 0, \tag{11b}$$

$$H' = G_c'' - G_c G_c' + \kappa\lambda Q_d(G_d - G_c), \tag{11c}$$

$$(G_d Q_d)' + F_d Q_d = 0, \tag{11d}$$

$$G_d F'_d + F_p^2 + \lambda(F_d - F_c) = 0 \qquad [11e]$$

and

$$G_d G'_d + \lambda(G_d - G_c) = -\epsilon H' \qquad [11f]$$

where a prime denotes differentiation with respect to η. By rewriting [11a–g] as seven first-order differential equations (shown in the appendix) it can be shown that [11a–g] is a seventh-order differential system. Seven appropriate boundary conditions are

$$F_c(0) = 1, \quad G_c(0) = 0, \qquad [12a, b]$$

$$F_c(\eta) \to 0, \quad F_d(\eta) \to 0, \quad G_d(\eta) \to G_c(\eta), \quad Q_d(\eta) \to 1, \quad H(\eta) \to 0 \quad \text{as} \quad \eta \to \infty, \qquad [12c–g]$$

where it has been assumed that the two phases are in equilibrium far from the sheet. It should be recognized that Q_d can be thought of as either a dimensionless particle-phase volume fraction or a dimensionless particle-phase in-suspension density. To be consistent with the terminology normally used in the literature in connection with the dusty-gas equations, Q_d will be hereafter referred to as a density.

In the next section an approximate closed-form solution of the dilute dusty-gas equations is found which illustrates the singularity discussed earlier in the context of the geometry chosen for the present investigation. Subsequent to that, numerical work is used to demonstrate that this singularity appears to be a feature of the dusty-gas model but not of the modified dusty-gas model associated with the exact form of [11a–g].

APPROXIMATE CLOSED-FORM SOLUTION

To motivate what follows consider [11f] evaluated at the sheet ($\eta = 0$). This equation has the form

$$G_d(0)(G'_d(0) + \lambda) = -\epsilon H'(0). \qquad [13]$$

If $\epsilon = 0$, this equation is satisfied by either

$$G_d(0) = 0 \qquad [14a]$$

or

$$G'_d(0) = -\lambda. \qquad [14b]$$

As will be shown subsequently, the singularity in the particle-phase density at the sheet appears to be associated with condition [14a]. It is clear that if $\epsilon \neq 0$, [14a] does not satisfy [13]. This suggests that the inclusion of the pressure-gradient term in [11f] may eliminate this singularity. The form of [13] is independent of the value of κ. This indicates that the existence of the singularity will not be affected by changes in κ. Both of these conjectures will be verified by later numerical work.

For the special case of $\kappa = 0$ [11a–c], governing the fluid-phase behavior, are uncoupled from [11d–f], governing the particle-phase behavior, and can be solved separately. Crane (1970) noticed that the solution of [11a, b] is

$$F_c = \exp(-\eta), \quad G_c = -1 + \exp(-\eta). \qquad [15a, b]$$

This solution can be used to illustrate some important features of the particle-phase behavior near the wall ($\eta \ll 1$). Attention will be confined to the case of $\kappa = 0$ in the following discussion so that this closed-form solution can be used.

Expending [15a, b] for small η and keeping only the first terms yields

$$F_c \doteq 1, \quad G_c \doteq -\eta. \qquad [16a, b]$$

To find a solution to [11d–f] valid for $\eta \ll 1$, it will be assumed that

$$F_d = C_1, \quad G_d = -C_2\eta, \quad Q_d = \frac{C_3}{\eta^\epsilon}. \qquad [17a–c]$$

Substituting [17a–c] into [11e, f] yields

$$C_1 = \frac{-\lambda \pm (\lambda^2 + 4\lambda)^{1/2}}{2} \qquad [18a]$$

and

$$C_2 = \frac{\lambda \pm (\lambda^2 - 4\lambda)^{1/2}}{2}. \qquad [18b]$$

As $\lambda \to \infty$, C_1 and C_2 must approach unity (equilibrium flow). Thus the positive sign in [18a] and the negative sign in [18b] must be selected to obtain

$$C_1 = \frac{\lambda\left[\left(1+\frac{4}{\lambda}\right)^{1/2} - 1\right]}{2} \qquad [19a]$$

and

$$C_2 = \frac{\lambda\left[1-\left(1-\frac{4}{\lambda}\right)^{1/2}\right]}{2}. \qquad [19b]$$

Since C_2 must be real, it can be seen that this solution exists only for $\lambda \geqslant 4$.

The analysis given above has determined the conditions ($\lambda \geqslant 4$) for which a solution satisfying [14a] is possible. Because the solution obtained through this analysis is purely local (in the vicinity of the sheet) there is no guarantee that a solution in the entire flow field which satisfies the boundary conditions at infinity can be found which will approach this local solution. For this particular problem, numerical solutions (see the next section) of [11f] (with $\epsilon = 0$) using [15b] to represent G_c show that for $\lambda \geqslant 4$, $G_d(0) = 0$. They further show that for $\lambda < 4$ $G_d(0) \neq 0$ and $G_d'(0) = -\lambda$. Thus, transition from condition [14a] to condition [14b] occurs at $\lambda = 4$. This is consistent with the local analysis but not proved by it. The sheet collects particles only below the critical value $\lambda_{cr} = 4$. This is typical of stagnation-point flows with the value of λ_{cr} depending on the body geometry and the assumed representation of the fluid-phase flow field [see, for instance, De la Mora (1982)].

Substitution of [17a–c] and [19a, b] into [11d] results in

$$e = 1 - \frac{\left[\left(1+\frac{4}{\lambda}\right)^{1/2} - 1\right]}{\left[1-\left(1-\frac{4}{\lambda}\right)^{1/2}\right]}. \qquad [20]$$

A check will show that for $\lambda \geqslant 4$, $0 \leqslant e \leqslant 2 - \sqrt{2} = 0.586$. Thus the solution for the particle-phase density possesses a singularity at $\eta = 0$. Again, this result is based on an approximate solution, but numerical solutions of [11d] appear to verify it (see the next section). This singularity was not noticed in early work on stagnation-point flows because the particle-phase density was not calculated.

As mentioned previously, all of the work discussed above is limited to the case of $\kappa = 0$ in order to utilize [15a, b]. Presumably the local analysis could be extended to arbitrary values of κ but, because of the limitations of such analysis, it does not seem worth while to do so.

NUMERICAL RESULTS AND DISCUSSION

Equations [11a–g] were solved numerically subject to [12a–g] by an iterative, variable-step-size, finite-difference technique. Three different versions of the method (corresponding to alternate ways of differencing some of the equations) were employed. It was found that all versions produced the same results. Much smaller step sizes were needed in the vicinity of the sheet to obtain accurate solutions of the two-phase equations than were required to solve the corresponding single-phase equations. This was the reason for employing a variable step size with the smallest step located at the sheet and the step size gradually increasing away from the sheet. For the sake of brevity the details of the numerical approach are omitted.

Numerical solutions of the dilute dusty-gas equations ($\kappa = \epsilon = 0$) were obtained first. The solutions of [11a, b] were compared to [15a, b] to verify the numerical work. Agreement between the exact and numerical solutions was found to be excellent. Solutions of the particle-phase equations showed that the particle-phase density at the sheet became increasingly large as λ was increased. It was found that for $\lambda < 4$ it was always possible to use a small enough step size so that $Q_d(0)$ became independent of the step size. For $\lambda > 4$, on the other hand, no such minimum step size could be found. That is, when a series of runs using successively smaller step sizes was made, reduction of the step size resulted in continuous growth of the particle-phase density at the sheet with the solution never becoming independent of the step size. This suggests that the particle-phase density is singular at the sheet, as was predicted by the approximate analytical solution.

Next the dusty-gas equations ($\epsilon = 0$) were numerically solved to determine whether they also exhibited singular behavior. No difficulty was encountered in obtaining solutions for $\lambda < 4$. For $\lambda > 4$ no solutions could be found which exhibited step-size independence. It appears, therefore, that use of the dusty-gas equations neither eliminates the singularity in the particle-phase density distribution nor alters the value of λ at which it first appears.

Finally, the complete equations [11a–g] (modified dusty-gas model) were solved. It was found that this removed the singularity in the particle-phase density distribution. Some of the results are presented in figures 1–10.

Typical computed results for the particle-phase density distribution are presented in figures 1 and 2. Figure 1 shows data for $\lambda = 3.5$, a value slightly smaller than $\lambda_{cr} = 4$. For $\epsilon = 0$ the approach of singular behavior is indicated by the large value of Q_d observed at the sheet. For finite values of ϵ, on the other hand, smaller values of $Q_d(0)$ are predicted. The decrease is dramatic. Away from the sheet the influence of ϵ is minimal. Figure 2 shows results for $\lambda = 10$, a value considerably larger than $\lambda_{cr} = 4$. The curve labeled $\epsilon = 0$ has no physical meaning in this case. It corresponds to a particular step size adjacent to the sheet of 0.002. Reductions in this step size were found to lead to increases in the value of $Q_d(0)$ with this quantity never becoming step-size independent. This indicated the presence of singular behavior. The curves labeled $\epsilon = 0.05$ and $\epsilon = 0.1$ are based on computations which were found to be step-size independent. They illustrate the ability of the modified dusty-gas model to predict finite values of particle-phase density at the sheet for all values of λ.

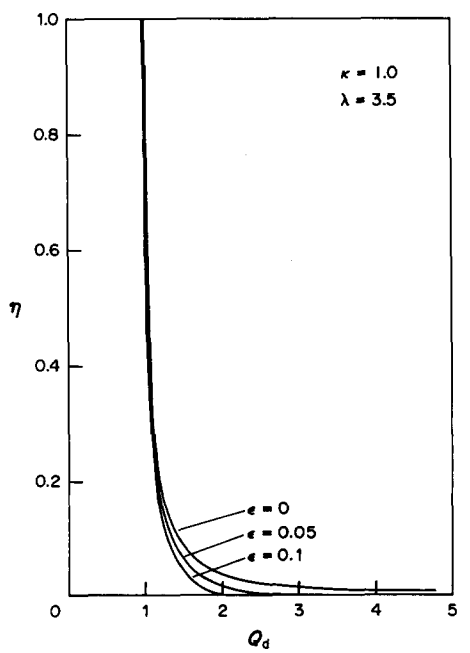

Figure 1. Particle-phase density profiles.

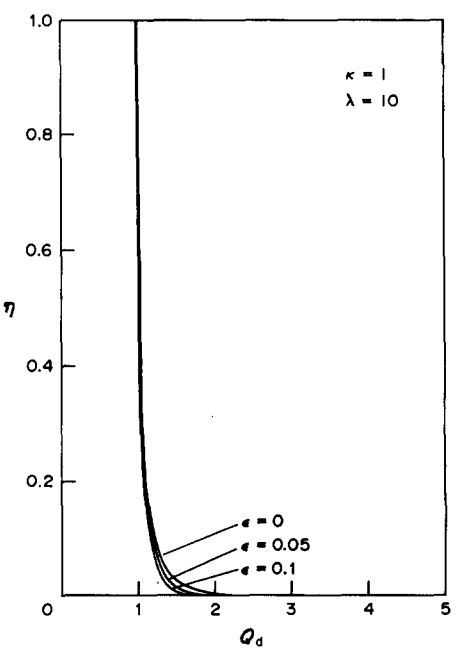

Figure 2. Particle-phase density profiles.

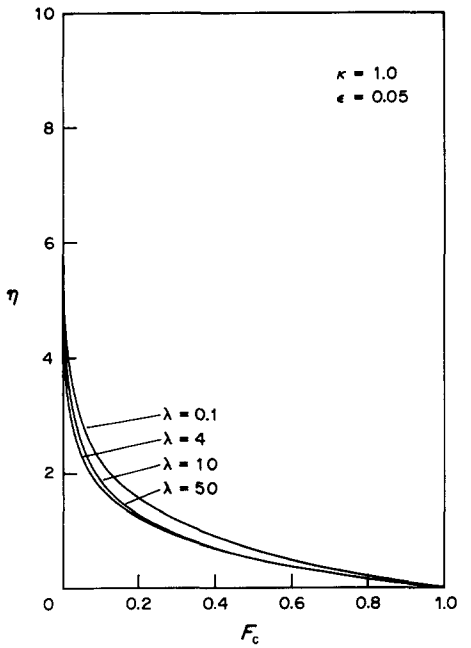

Figure 3. Fluid-phase tangential velocity profiles.

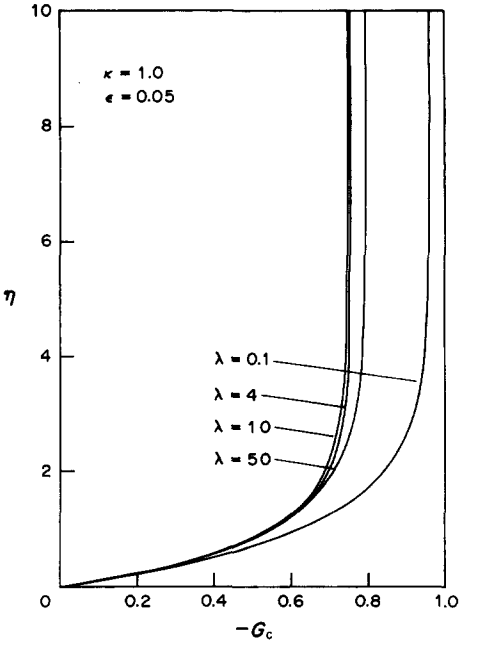

Figure 4. Fluid-phase normal velocity profiles.

In contrast to the situation discussed above, it was found that the corresponding predictions for the velocity components and pressure were virtually insensitive to the value of ϵ. For the sake of brevity, these results are not shown graphically.

Figures 3–8 show the velocity, pressure and density distributions for a wide range of λ. These results illustrate the ability of the modified dusty-gas model to predict solutions over the entire range of λ. In particular, figure 7 shows that the particle-phase density increases as λ increases toward $\lambda_{cr} = 4$ then decreases as λ grows larger than 4. Thus the particle-phase density is uniform in both the frozen ($\lambda \ll 1$) and equilibrium ($\lambda \gg 1$) limits as it should be for this problem.

Figures 9 and 10 present plots of the quantity $-G_d(0)Q_d(0)$ vs λ for various density ratios. This quantity is a measure of the collection efficiency of the sheet. This can be seen as follows. The

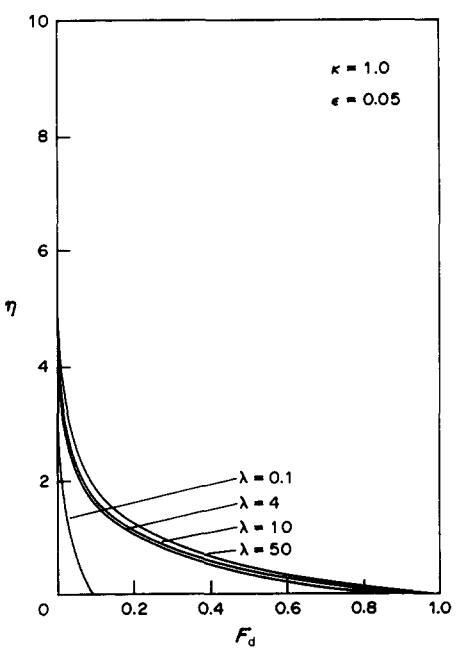

Figure 5. Particle-phase tangential velocity profiles.

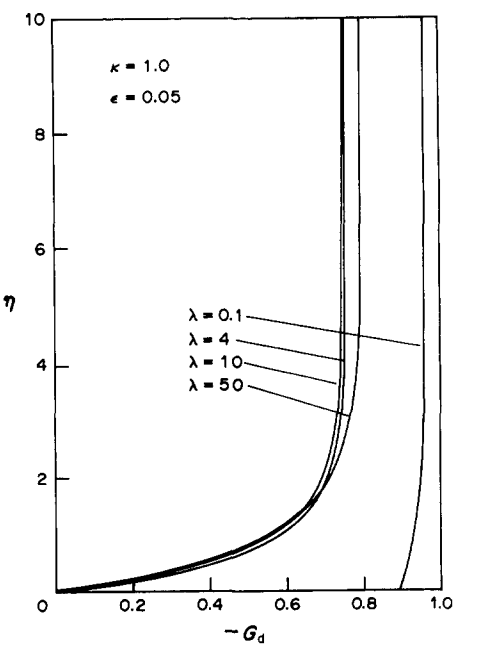

Figure 6. Particle-phase normal velocity profiles.

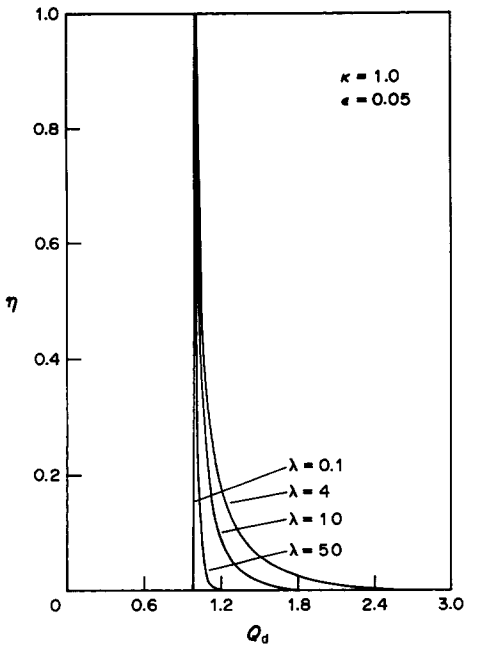

Figure 7. Particle-phase density profiles.

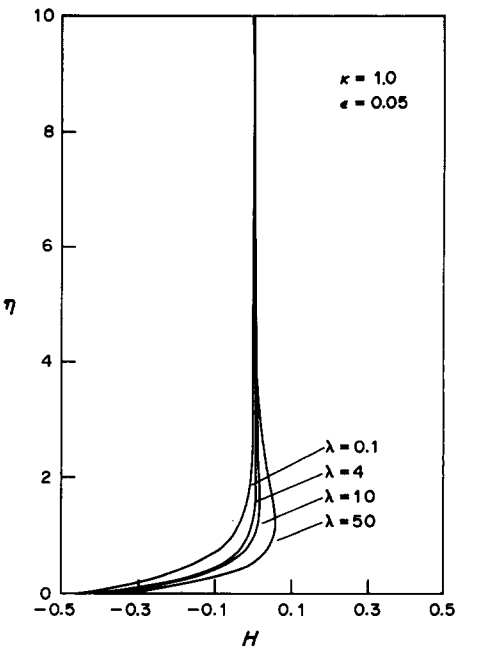

Figure 8. Fluid-phase pressure profiles.

quantity $-G_d(0)Q_d(0)$ is the actual dimensionless mass flux of particles striking the sheet. If the particles were totally unaffected by the presence of the fluid ($\lambda = 0$), the corresponding values would be $G_d(0) = -1$ and $Q_d(0) = 1$, which would yield $-G_d(0)Q_d(0) = 1$. Thus $-G_d(0)Q_d(0)$ is the ratio of the actual mass flux of particles striking the sheet to the mass flux of particles which would strike the sheet in absence of interaction between the fluid and particle phases. This is the usual definition of collection efficiency.

From figures 9 and 10 it can be seen that the collection-efficiency predictions based on the dusty-gas model are qualitatively correct but underpredict the refined values based on the modified

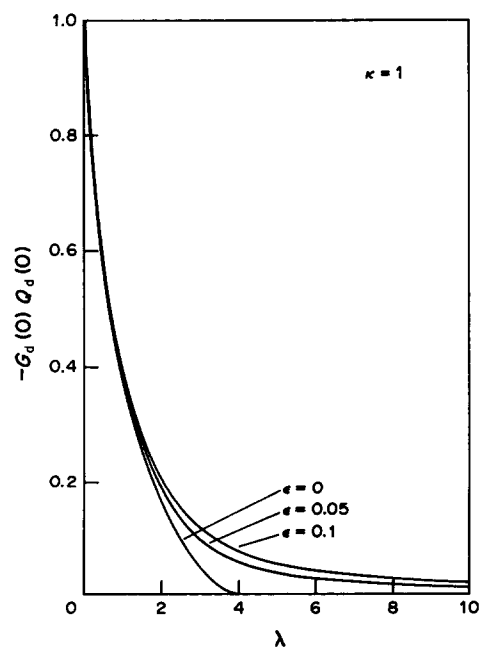

Figure 9. Collection efficiency vs inverse Stokes number.

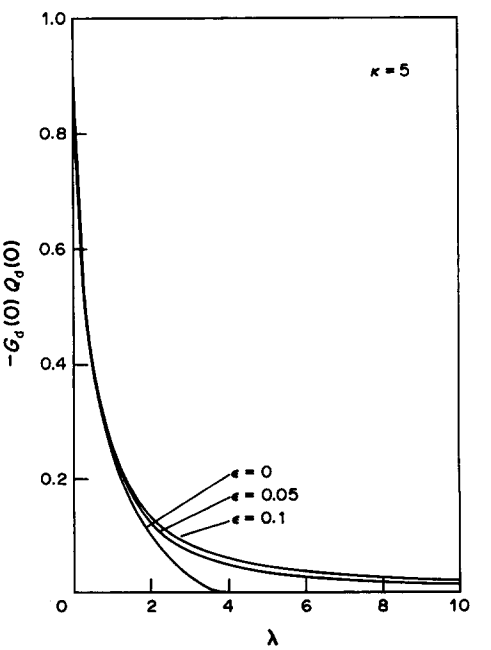

Figure 10. Collection efficiency vs inverse Stokes number.

dusty-gas model, with the difference increasing with λ and becoming especially noticeable for $\lambda > 4$. Since singular behavior is absent in the modified dusty-gas predictions, the collection efficiency slowly decreases to zero as λ increases, rather than vanishing abruptly at $\lambda = 4$. It is believed that the results presented graphically in figures 9 and 10 may be the first to show this behavior.

It should be mentioned that the numerical results presented in figures 1–10 constitute only a small portion of the data computed in the course of the present work. They were chosen as representative of trends observed in a variety of calculations. All numerical work was confined to small values of ϵ (appropriate for suspensions of solid particles or liquid drops in gases.) For larger values of ϵ, it would probably be necessary to include additional terms in [6a–d] (added mass etc.) to get a realistic model. For this reason only small values of ϵ were considered.

CONCLUSION

This paper discussed two-dimensional steady flow containing a stagnation point generated by a stretching infinite sheet which bounds a half space of a two-phase particulate suspension. The balance equations for mass and linear momentum were combined with appropriate constitutive equations, expressed in component form, nondimensionalized and reduced to ordinary differential equations. The resulting nonlinear coupled equations were solved numerically by an iterative finite-difference method. Representative results of the computations were presented graphically and used to illustrate various interesting features of the solutions. Analysis of the computed results led to several conclusions. These are summarized below.

First, numerical solutions of the dilute dusty-gas equations indicate the presence of a singularity in the particle-phase density above a critical value of the interphase momentum-transfer parameter (inverse Stokes number) λ. The singularity occurs at the fluid-phase stagnation point. The critical value of λ appears to be 4. Thus the numerical solutions confirm the predictions of an approximate closed-form solution which is valid locally in the vicinity of the stagnation point.

Second, numerical solutions of the dusty-gas equations indicate the presence of a singularity in the particle-phase density qualitatively similar to the one discussed above. The location and the critical value of the inverse Stokes number do not appear to be significantly affected.

Third, generalization of the dusty-gas model to include the influence of the fluid-phase pressure gradient on the particle-phase momentum balance (i.e. use of the modified dusty-gas model) eliminates the singularity discussed above. This is because the effect of the pressure gradient is to apply an additional force to the particle phase which, in the vicinity of the sheet, is directed toward the sheet. This prevents the particle-phase normal velocity from vanishing at the sheet which, in turn, prevents the particle-phase density from becoming infinite at the sheet. For inverse Stokes numbers less than the critical value numerical work indicates that predictions based on the original and modified dusty-gas models are very similar. With the modified dusty-gas model it is possible to compute solutions over the entire range of inverse Stokes numbers. These solutions have the correct qualitative behavior. In particular, the particle-phase density distribution shows the proper progression from uniformity at $\lambda = 0$ to maximum nonuniformity at $\lambda = 4$ to uniformity at $\lambda = \infty$. Collection-efficiency calculations based on the modified dusty-gas model indicate that previously reported collection-efficiency results, obtained through the use of the dusty-gas model, are qualitatively correct. Both are in excellent agreement for $\lambda < 4$. For $\lambda > 4$ the modified model predicts a small collection efficiency while the original model predicts this to be zero.

Some tentative comments concerning two-phase stagnation-point flows can be made based on the model problem discussed herein. First, it is not necessary to abandon the "dusty-gas" (small volume fraction, finite particle loading) concept to eliminate singular behavior in the particle-phase density. Inclusion of a pressure-gradient term in the particle-phase momentum-balance equation is sufficient to do that. Second, inclusion of the interphase momentum-transfer term in the fluid-phase momentum-balance equation (the neglect of which is obviously incorrect when the particle-phase density becomes sufficiently large) is not enough, by itself, to eliminate singular behavior in the particle-phase density. Third, use of the modified dusty-gas equations discussed in this paper is only one way to eliminate this singularity. Other methods should be investigated so that the most realistic model can be found.

REFERENCES

CRANE, L. J. 1970 Flow past a stretching plate. *Z. angew. Math. Phys.* **21,** 645–647.

DE LA MORA, J. & ROSNER, D. E. 1981 Inertial deposition of particles revisited and extended: Eulerian approach to a traditionally Lagrangian problem. *PhysicoChem. Hydrodynam.* **2,** 1–21.

DE LA MORA, J. 1982 Two dimensional stagnation point flow of a dusty gas near an oscillating plate. *Acta mech.* **43,** 261–265.

MARBLE, F. E. 1970 Dynamics of dusty gases. *A. Rev. Fluid Mech.* **2,** 397–446.

MICHAEL, D. H. 1968 The steady motion of a sphere in a dusty gas. *J. Fluid Mech.* **31,** 175–192.

PEDDIESON, J. 1973 On predicting the collection efficiencies of fibrous filters. *Rec. Adv. Engng Sci.* **7,** 309–316.

PEDDIESON, J. 1976 Analysis of dust collection problems. *Dev. theor. appl. Mech.* **8,** 539–564.

TAYLOR, G. I. 1940 Notes on possible equipment and technique for experiments on icing of aircraft. Technical Report 2024, Aeronautical Research Committee.

UNGARISH, M. & GREENSPAN, H. P. 1983 On two-phase flow in a rotating boundary layer. *Stud. appl. Math.* **69,** 145–175.

ZUNG, L. B. 1969 Flow induced in a fluid–particle suspension by an infinite rotating disk. *Phys. Fluids* **12,** 18–23.

APPENDIX

By defining $E_c = F_c'$, [11a–g] can be rewritten in the equivalent form,

$$E_c' = G_c F_c + F_c^2 + \kappa\lambda Q_d (F_c - F_d), \tag{A.1a}$$

$$F_c' = E_c, \tag{A.1b}$$

$$G_c' = -F_c, \tag{A.1c}$$

$$H' = -E_c + G_c F_c + \kappa\lambda Q_d (G_d - G_c), \tag{A.1d}$$

$$F_d' = \frac{-F_d^2 + \lambda(F_d - F_c)}{G_d}, \tag{A.1e}$$

$$G_d' = \frac{\epsilon(E_c - G_c F_c) + \lambda(1 + \kappa\epsilon Q_d)(G_c - G_d)}{G_d} \tag{A.1f}$$

and

$$Q_d' = \frac{-Q_d\left[\dfrac{\epsilon(E_c - G_c F_c) + \lambda(1 + \kappa\epsilon Q_d)(G_c - G_d)}{G_d + F_d}\right]}{G_d}. \tag{A.1g}$$

These are seven first-order equations, or a seventh-order system.